THE JOURNAL OF BIOLOGICAL CHEMISTRY VOL. 287, NO. 51, pp. 42773–42783, December 14, 2012

Human Exonuclease 5 Is a Novel Sliding Exonuclease Required for Genome Stability*

Received for publication, September 24, 2012, and in revised form, October 19, 2012 Published, JBC Papers in Press, October 24, 2012, DOI 10.1074/jbc.M112.422444

Justin L. Sparks[‡], **Rakesh Kumar**[§], **Mayank Singh**[§], **Marc S. Wold**[¶], **Tej K. Pandita**[§1], **and Peter M. Burgers**[‡2]

From the [‡]*Department of Biochemistry and Molecular Biophysics, Washington University School of Medicine, St. Louis, Missouri 63110,* [§]*Department of Radiation Oncology, University of Texas Southwestern Medical Center, Dallas, Texas 75390, and* [¶]*Department of Biochemistry, University of Iowa Carver College of Medicine, Iowa City, Iowa 52242*

Background: Deoxyribonucleases are key DNA metabolic enzymes, but their functions remain ill defined.
Results: Human EXO5 is a novel bidirectional single strand-specific sliding exonuclease; however, RPA enforces a 5′-directionality of nuclease activity.
Conclusion: hEXO5 functions in nuclear genome maintenance and interstrand cross-link repair.
Significance: Nucleases are important in directing pathway choices at DNA damage and replication blocks.

Previously, we characterized *Saccharomyces cerevisiae* exonuclease 5 (*EXO5*), which is required for mitochondrial genome maintenance. Here, we identify the human homolog (C1orf176; *EXO5*) that functions in the repair of nuclear DNA damage. Human EXO5 (hEXO5) contains an iron-sulfur cluster. It is a single-stranded DNA (ssDNA)-specific bidirectional exonuclease with a strong preference for 5′-ends. After loading at an ssDNA end, hEXO5 slides extensively along the ssDNA prior to cutting, hence the designation sliding exonuclease. However, the single-stranded binding protein human replication protein A (hRPA) restricts sliding and enforces a unique, species-specific 5′-directionality onto hEXO5. This specificity is lost with a mutant form of hRPA (hRPA-t11) that fails to interact with hEXO5. hEXO5 localizes to nuclear repair foci in response to DNA damage, and its depletion in human cells leads to an increased sensitivity to DNA-damaging agents, in particular interstrand cross-linking-inducing agents. Depletion of hEXO5 also results in an increase in spontaneous and damage-induced chromosome abnormalities including the frequency of triradial chromosomes, suggesting an additional defect in the resolution of stalled DNA replication forks in hEXO5-depleted cells.

Exonucleases are versatile processors of metabolic intermediates during DNA metabolism involving replication and recombination and the various pathways that function during the response to DNA damage in the cell (1). By definition, exonucleases need a DNA end for activity, and the vast majority generates mononucleotides as the products of nuclease action. However, some exonucleases with specialized functions can cut internally of the DNA end that they initially engage. An example is the flap exonuclease Fen1 that cuts precisely at the base of a 5′-flap after having loaded at the 5′ terminus during the process of Okazaki fragment maturation (2, 3). The novel exonuclease described in this study, human EXO5 (hEXO5),[3] loads at ssDNA ends and then slides along the ssDNA prior to cutting (sliding exonuclease). Our studies suggest that hEXO5 functions in the repair of DNA damage, in particular ultraviolet (UV) irradiation and interstrand cross-link (ICL) damage.

Interstrand cross-links are genotoxic lesions that covalently link the two strands of the DNA duplex together. DNA strand separation is an essential step in the processes of DNA metabolism including transcription, replication, and recombinational repair. Interstrand cross-links create complete obstructions of these fundamental DNA metabolic processes, leading to potent genotoxicity. Importantly, ICLs can arise from exogenous agents such as the anticancer drugs cisplatin and mitomycin C (MMC) and endogenous sources in the form of by-products of metabolic processes (4). In general, these agents also form intrastrand cross-links (5). However, the interstrand cross-links are generally considered to be much more genotoxic. ICL repair predominantly occurs during S phase while DNA replication takes place and is initiated by the convergence of replication forks at sites of ICLs (6).

Here, we describe the biochemical properties and biological function of a novel human bidirectional exonuclease, which is a sequence homolog of *Saccharomyces cerevisiae* Exo5 that we characterized previously as an exonuclease essential for mitochondrial genome maintenance (7). However, through a fascinating turn of evolutionary events, it appears that the distinct mitochondrial function of Exo5 prevails only in the Saccharomycetales order of fungi because they possess a strong mitochondrial localization signal. Other fungi and organisms including mammals lack such a localization signal and may have dedicated Exo5 to the task of maintaining nuclear genome stability (see Fig. 1*A*). All members of the Exo5 family share some common characteristics beyond that of primary amino acid sequence. They possess an iron-sulfur cluster that is structurally important in linking the N terminus to the C terminus of

* This work was supported, in whole or in part, by National Institutes of Health Grants GM032431 and GM083970 (to P. M. B.); CA123232, CA129537, CA154320, and U19A1091175 (to T. K. P.); and GM44721 (to M. S. W.).
[1] To whom correspondence may be addressed. Tel.: 214-648-1918; Fax: 214-648-4995; E-mail: tej.pandita@utsouthwestern.edu.
[2] To whom correspondence may be addressed. Tel.: 314-362-3872; Fax: 314-372-7183; E-mail: burgers@biochem.wustl.edu.

[3] The abbreviations used are: hEXO5, human EXO5; Exo5, exonuclease 5; ssDNA, single-stranded DNA; RPA, replication protein A; hRPA, human replication protein A; ICL, interstrand cross-link; MMC, mitomycin C; mEXO5, mouse EXO5.

the enzyme, thereby likely creating a cavity that may encircle the ssDNA. A similar structural motif was previously identified in the *Bacillus subtilis* recombinase AddAB (8). However, our study shows that the detailed biochemical properties of hEXO5 are quite different from those of the budding yeast enzyme, and this may reflect their distinct functions in the nucleus *versus* mitochondrion, respectively. Depletion of hEXO5 in human 293 cells leads to hypersensitivity to genotoxic agents including UV irradiation and particularly to ICL-inducing agents. However, sensitivity to ionizing radiation exposure was not observed in hEXO5-depleted cells. Depletion of hEXO5 also leads to the accumulation of a higher percentage of chromosome aberrations either spontaneously or after treatment with cross-linking agents. In particular, an accumulation of triradial chromosomes was observed at metaphase that is indicative of unresolved and collapsed replication forks (9). These biochemical and genetic results suggest that hEXO5 plays a role in genome stability in general.

EXPERIMENTAL PROCEDURES

Plasmids and Oligonucleotides—Plasmid pBL277 contains the *Schistosoma japonicum* glutathione *S*-transferase (GST) gene fused to the N terminus of the human *EXO5* (C1orf176) gene in vector pRS424-GALGST (10). The GST tag is separated from the N terminus of hEXO5 by a recognition sequence for the human rhinoviral 3C protease (LEVLFQ ↓ GP). Following cleavage by the protease, the N-terminal sequence of hEXO5 is extended with the GPEF sequence. All variants and mutants were made in pBL277. Plasmid pBL276 contains the GST tag fused to the N-terminal 220-amino acid domain of the *Escherichia coli* GyrB gene (11) followed by a six-amino acid linker fused to the N terminus of hEXO5. Plasmid pBL272 is a plasmid for mammalian expression with a C-terminal GFP-hEXO5 construct. Plasmids and sequences are available upon request.

The following oligonucleotides were purchased from Integrated DNA Technologies, *Inc.* (Coralville, IA) and purified by urea-polyacrylamide gel electrophoresis (PAGE): c81, TTGCCGATGAACTTTTTTTTTGATCGAGAC CTT; v81, AAGGTCTCCATCAAAAAAAAAAGTTCATCGGCAA. The polarity switch oligonucleotides were a gift from Dr. Timothy Lohman. The 5′-^{32}P label was introduced on oligonucleotides using [γ-^{32}P]ATP and T4 polynucleotide kinase, whereas the 3′-^{32}P label was introduced by incubation with [α-^{32}P]dATP and terminal deoxynucleotidyltransferase under the manufacturers' recommended conditions. Labeled oligonucleotides were hybridized with a 3-fold excess of the relevant complimentary oligonucleotide. Labeled c81 was circularized first by hybridization with equimolar bridging oligonucleotide circ81 (ATCGGCAAAAGGTCTC) followed by ligation with T4 DNA ligase and urea-PAGE purification.

EXO5 Overproduction and Purification—EXO5 overproduction was carried out in *S. cerevisiae* strain FM113 (MAT**a** *ura-3-52 trp1-289 leu2-3112 prb1-1122 prc1-407 pep4-3*) transformed with plasmid pBL277 (hEXO5) or pBL282 (mouse EXO5 (mEXO5)). Growth, induction, extract preparation, and ammonium sulfate precipitation (0.3 g/ml) were similar to the procedures described previously (12). The precipitate was dissolved in buffer A_0 (buffer A, 60 mM HEPES-NaOH (pH 7.8), 10% glycerol, 1 mM dithiothreitol (DTT), 0.1 mM EDTA, 0.005% polyoxyethylene (10) lauryl ether, 5 mM sodium bisulfite, 5 μM pepstatin A, and 5 μM leupeptin; subscript number indicates the mM sodium acetate concentration) until the lysate conductivity was equal to that of buffer A_{400}. The lysate was then used for batch binding to 1 ml of glutathione-Sepharose 4B beads (GE Healthcare), equilibrated with buffer A_{400}, and gently rotated at 4 °C for 2 h. The beads were collected at 1,000 rpm in a swinging bucket rotor followed by batch washes (3 × 20 ml of buffer A_{400}). The beads were transferred to a 10-ml column and washed at 2.5 ml/min with 100 ml of buffer A_{400}. The second wash was with 50 ml of buffer A_{400} containing 5 mM magnesium acetate and 1 mM ATP, and the third wash used 50 ml of buffer A_{400} and 30 ml of buffer A_{200}. Elution was carried out at a flow rate of 0.2 ml/min with buffer A_{200} containing 20 mM glutathione (pH adjusted to 8.0). Fractions containing EXO5 were combined and diluted with buffer A_0 to equal buffer A_{100} and then loaded onto a 1-ml Mono Q column. Protein was eluted with a linear gradient of buffer A_{100} to A_{1200}. The fractions containing pure protein were incubated overnight at 4 °C with 30 units of rhinoviral 3C protease, diluted with A_0 to equal A_{100}, and loaded onto a 1-ml Mono Q column. Pure EXO5 protein was eluted at 300–400 mM sodium acetate. mEXO5 and hEXO5 variants and mutants were overexpressed and purified similarly.

Analytical Ultracentrifugation—Purified protein was dialyzed against a buffer of 30 mM HEPES (pH 7.4), 100 mM sodium acetate, 5% glycerol, and 5 mM β-mercaptoethanol overnight at 0 °C. We used a Beckman Optima XL-A analytical ultracentrifuge and ran a velocity experiment at 40,000 rpm for 6 h with 5 μM hEXO5. The traces were analyzed using the Sedfit program.

Exonuclease Assays—The standard 10-μl assay mixture contained 100 mM Tris-HCl (pH 7.8), 500 μg/ml bovine serum albumin, 5 mM DTT, 5 mM magnesium acetate, 50 mM NaCl, 50–100 fmol of ^{32}P-end-labeled oligonucleotide substrate, and enzyme. Incubations were carried out at 30 °C for the indicated time periods. Deviations from the standard assay conditions are indicated in the legends of the figures. Reactions were stopped with 10 mM final concentration of EDTA in addition to 40% formamide and analyzed by 7 M urea-18% PAGE. Dried gels were subjected to phosphorimaging analysis.

Forced Dimerization Assay—The standard 10-μl assay mixture was the same as for the standard exonuclease assay; however, all assays were carried out under initial linear rate conditions in which <30% of the substrate was hydrolyzed. Coumermycin (Sigma-Aldrich) was dissolved in DMSO and further diluted in H_2O, and novobiocin (Sigma-Aldrich) was dissolved in H_2O. Reactions were stopped as described above. The reactions were analyzed by 7 M urea-18% PAGE. Dried gels were analyzed by phosphorimaging.

Electrophoretic Mobility Shift Assay (EMSA)—The standard 20-μl EMSA assay mixture contained 100 mM Tris-HCl (pH 7.8), 500 μg/ml bovine serum albumin, 5 mM DTT, 1 mM EDTA, 50 mM NaCl, 20% glycerol, 50 fmol of ^{32}P-end-labeled oligonucleotide substrate or unlabeled oligonucleotide, and enzyme. Incubations were carried out at 25 °C for the indicated periods. Reactions were loaded on 5% non-denaturing polyacrylamide gels prerun for 2 h at 4 °C. Either gels were dried and

subjected to phosphorimaging analysis, or the proteins were transferred to nitrocellulose for Western analysis with rabbit antibodies to hEXO5. Deviations from the standard assay conditions are indicated in the legends to the figures.

Human Cell Growth and Transfection—Human 293 and GM5849 cells were maintained by previously published procedures (13). Full-length FLAG-tagged hEXO5 cDNA cloned in pcDNA3.1 was transfected into cells. hEXO5 small interfering RNA (siRNA) and control luciferase siRNA were obtained from Integrated DNA Technologies, *Inc.* or Dharmacon Research (Lafayette, CO). The hEXO5 siRNAs were as follows: ORF176-1, ACUCAGAACUGGUGUGAACUU + GUUCACACCAGUUCUGAGUUU; ORF176-2, CUGUGAAGUCUUUGGGUGAUU + UCACCCAAAGACUUCACAGUU. RNA interference (RNAi) treatment of 293 cells was performed as described previously (14). Cells were used 72 h after transfection for all experimental purposes.

Human Damage Sensitivity Assays—Clonogenic survival was determined using human 293 cells. Cells after 72 h of transfection with control or hEXO5 siRNA were seeded at known densities onto 60-mm dishes in 5.0 ml of medium, incubated for 16 h, and washed with 1× phosphate-buffered saline (PBS) prior to UV or ionizing radiation or exposure to the indicated doses of mitomycin C for 24 h or cisplatin for 1 h. Cells were washed and incubated in fresh medium for ~12 days and then fixed in methanol-acetic acid (3:1) prior to staining with crystal violet. Only colonies containing >50 cells were counted. Each experiment was repeated three to four times. The S.E. is given in the figures. Chromosome aberrations were analyzed at metaphases, which were prepared by standard procedures (15, 16). Cells were treated with cisplatin or mitomycin C, and metaphases were collected after different time points of drug treatment.

Immunostaining—Cells grown in chamber slides were exposed to irradiation (10 J/m^2) and incubated at 37 °C prior to fixation. Cells were fixed in 2% paraformaldehyde for 15 min, washed in 1× PBS, permeabilized for 5 min on ice in 0.2% Triton X-100, and blocked in PBS with 1% bovine serum albumin. The procedure used for immunostaining is the same as that described previously (17–19).

RESULTS

hEXO5 Contains a Conserved Iron-Sulfur Cluster—The catalytic domain of eukaryotic Exo5 is distantly related to the *E. coli* RecB nuclease domain of the bacterial RecBCD recombinases (Fig. 1, *B* and *C*) (8). We recently reported that *S. cerevisiae EXO5* is essential for mitochondrial genome maintenance (7). However, a phylogenetic and cellular localization prediction analysis of 95 eukaryotic Exo5 proteins indicates that strong mitochondrial localization prevails only in the Saccharomycetales order of fungi (Fig. 1*A*). This phylogenetic analysis along with our biochemical and functional cellular studies suggests that in other fungi and in metazoans Exo5 has a role in maintaining nuclear genome stability. Therefore, we carried out a biochemical and genetic analysis of hEXO5. The cDNA for human C1orf176 was cloned, and the gene was designated *EXO5*. hEXO5 with an N-terminal GST tag was overexpressed in a yeast overexpression system, and the recombinant protein was purified to apparent homogeneity by a combination of affinity and ion exchange chromatography (see "Experimental Procedures"). An analysis of hEXO5 by analytical ultracentrifugation showed that the protein exists in a monomeric form (Fig. 1*D*). The homolog from *Mus musculus* (RP23-182D20.4, *Exo-5*) was also cloned, and the enzyme was purified analogously (data not shown).

Upon purification of hEXO5, we noticed that it was yellow-brown in color, suggesting the presence of an iron-sulfur cluster. Indeed, the UV-visible spectrum of hEXO5 showed a peak at 410 nm, indicative of the presence of an iron-sulfur cluster, most likely of the [4Fe-4S] form (Fig. 1*E*). From aligning several Exo5 homologs, we noticed a set of four conserved cysteine residues, one N-terminal with respect to the catalytic core and three C-terminal of the catalytic core. This is a unique arrangement for coordination of the Fe-S cluster that was previously identified in the *B. subtilis* AddB helicase-nuclease (Fig. 1*C*) (8). This arrangement is conserved in mEXO5, which also purifies as a yellow protein with a UV-visible peak at 410 nm. To test whether the conserved cysteines are responsible for coordination of the iron-sulfur cluster, we purified a hEXO5 form with cysteines at 343 and 346 mutated to alanines (hEXO5-CCAA), and the mutant hEXO5 protein was colorless and lacked absorption at 410 nm (Fig. 1*E*). Lack of the iron-sulfur cluster also led to an 80–90% loss of catalytic activity of hEXO5, indicating that this structural motif is important but not essential for enzymatic function (Fig. 1*G*).

Both human and mouse EXO5 degraded ssDNA; however, their activities were both quite low with turnover numbers in the order of min^{-1} (Fig. 1*F*). When mammalian Exo5 was overexpressed in *E. coli*, the persistent presence of contaminating *E. coli* nucleases made a reliable characterization problematic (data not shown). Therefore, we exploited the yeast overexpression system (described under "Experimental Procedures"), which dramatically reduced the level of contaminating nuclease activities. Considering the very low catalytic activity of hEXO5, it was important to establish that the observed activity was not caused by a contaminating yeast nuclease. Based upon the alignment with the RecB nuclease domain (20), we predicted that Asp-182 and Glu-196 bind the divalent metal ion that is essential for catalysis (Fig. 1, *B* and *C*). The E196A form of hEXO5 was purified and shown to display negligible nuclease activity (<1% of wild type), indicating that the observed wild-type activity albeit low is valid (Fig. 1*G*). We also purified two naturally occurring variants of hEXO5, either with a D115N or V172G change, and these variants had activity similar to that of the reference hEXO5 (Asp-115 and Val-172), which we designate as wild type (Fig. 1*G*). Below we explore the basis for the low enzymatic activity of mammalian Exo5.

The Exo5 Orthologs Are Sliding Bidirectional Exonucleases—A variety of oligonucleotide structures were analyzed as substrates for hEXO5. The enzyme is specific for DNA as single-stranded RNA was not degraded (data not shown). DNA structures such as Holliday junctions, replication forklike structures, and DNA flap substrates showed no activity unless these structures contained a free ssDNA tail, and none of these structures showed a higher activity than a simple ssDNA substrate did (Fig. 2, *A* and *C*, and data not shown). Thus, hEXO5 is a

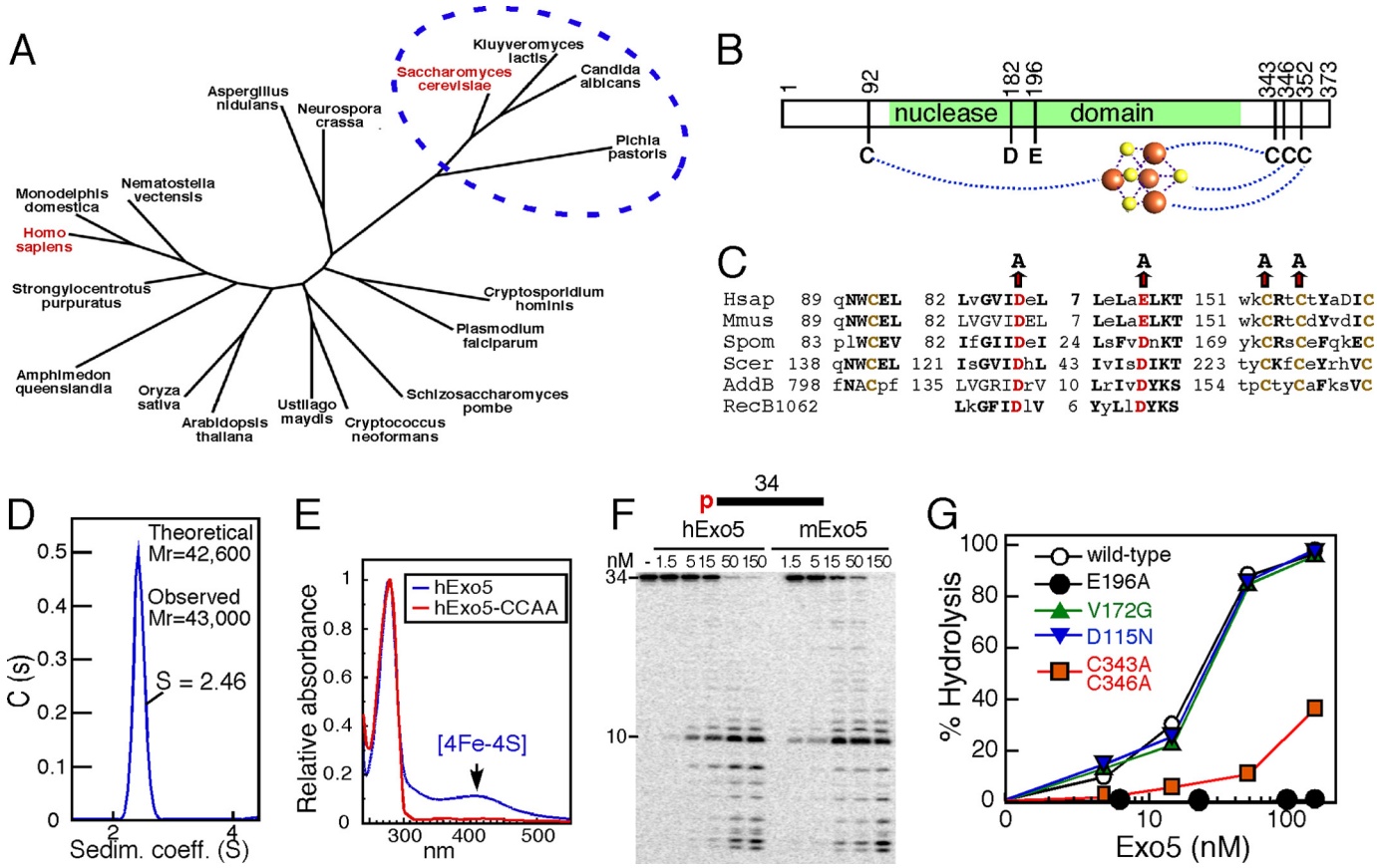

FIGURE 1. **Catalytic activity of hEXO5.** *A*, phylogenetic analysis. Using PSI-BLAST, 108 eukaryotic Exo5 sequences were identified in GenBank. This set was culled by imposing the following requirements: (i) an N-terminal methionine and (ii) the diagnostic WCE and CX_2CX_5C motifs N-terminal and C-terminal of the catalytic domain that constitute the iron-sulfur cluster coordinating cysteines. The remaining 95 sequences were subjected to PREDOTAR to identify classical N-terminal mitochondrial localization sequences and to Phylogeny.fr for phylogenetic analysis using MUSCLE multiple alignment and PhyML phylogeny analysis. All 15 Saccharomycetales Exo5 proteins showed a medium to strong mitochondrial localization probability (0.2–0.92). The mitochondrial localization probability of all 80 other Exo5 proteins was 0–0.02 with the exception of *Zea mays* (0.25) and *Strongylocentrotus purpuratus* (0.28). A tree of 18 representative model organisms is shown. *B*, schematic representation of the domain architecture of hEXO5 with conserved active site residues and iron-sulfur coordinating cysteine residues indicated. *C*, sequence alignment of critical residues in the Exo5 family. Active site Asp/Glu are shown in *red*, Gln and Tyr of a highly conserved α helix are shown in *green*, and four conserved Cys residues that coordinate the Fe-S cluster are shown in *brown*. *Hsap*, *Homo sapiens*; *Mmus*, *M. musculus*; *Spom*, *S. pombe*; *Scer*, *S. cerevisiae*; *RecB*, nuclease domain of *E. coli* RecBCD recombinase; *AddB*, nuclease domain of *B. subtilis* AddAB recombinase. *D*, purified hEXO5 (5 μM) in buffer containing 100 mM sodium acetate was run in a Beckman Optima XL-A analytical ultracentrifuge as described under "Experimental Procedures." *Sedim. coeff.*, sedimentation coefficient. *E*, UV spectrum of hEXO5 and the C143A,C146A (*CCAA*) mutant. Traces were set to 1.0 at 279 nm. *F*, activity of hEXO5 variants and mutants. Standard assay mixtures used 10 nM 5′-labeled 34-nucleotide DNA substrate. The concentrations of the hEXO5 from *left* to *right* are 5, 15, 50, and 150 nM. The reactions were carried out at 30 °C for 4 min. The results were analyzed on a 7 M urea-18% polyacrylamide gel. *G*, the indicated hEXO5 mutant proteins were purified as described for the wild type, and standard nuclease assays with increasing concentrations of protein were carried out for 4 min at 30 °C.

single strand-specific deoxyribonuclease, and fully double-stranded DNAs (dsDNAs) are resistant to degradation (Fig. 2*A*, *lanes 5–7 versus 11–13*). The enzyme also requires a free DNA end for activity as the circularized form of the single-stranded oligonucleotide was not cleaved (*lanes 8–10*).

To determine whether hEXO5 is a 5′- or 3′-exonuclease, we utilized an ssDNA substrate hybridized with a 12-nucleotide complementary oligonucleotide to form a dsDNA block at either the 5′-end or the 3′-end. Although the 5′-blocked substrate showed a large decrease in activity (Fig. 2*A*, *lanes 14–16*), the 3′-blocked substrate showed only marginal inhibition (*lanes 17–19*), suggesting that hEXO5 is primarily a 5′-exonuclease, but it may also have 3′-exonuclease activity (Fig. 2*B*). We designed two partially double-stranded oligonucleotides with either a 5′- or 3′-ss-$(dT)_{25}$ flap (Fig. 2*C*). Both the 5′- and 3′-flap substrates were degraded by hEXO5 with the 5′-flap substrate being the preferred substrate. These data suggest that hEXO5 is a bidirectional single strand-specific exonuclease with a preference for 5′-ends. However, an alternative explanation that the enzyme slides onto the dsDNA ends of the flap substrates prior to cutting into the ssDNA region could not be excluded by these experiments.

To test the exonuclease polarity problem in an unambiguous manner, we used a set of oligo(dT) substrates in which the chain polarity is switched in the middle of the oligonucleotide by either a 3′-3′- or 5′-5′-dinucleotide linkage so that the resulting oligo(dT) has either two 5′- or two 3′-ends, respectively (Fig. 2*D*). The use of homopolymeric oligo(dT) substrates also eliminates potential problems in activity relating to sequence context (Fig. 2*A*) or secondary structure formation. Control studies showed that the proofreading 3′-exonuclease activity of DNA polymerase δ degraded the substrate with only 3′-ends but not the substrate with only 5′-ends (Fig. 2*D*). Conversely, λ-exonuclease, a 5′-nuclease, degraded the substrate with only 5′-ends

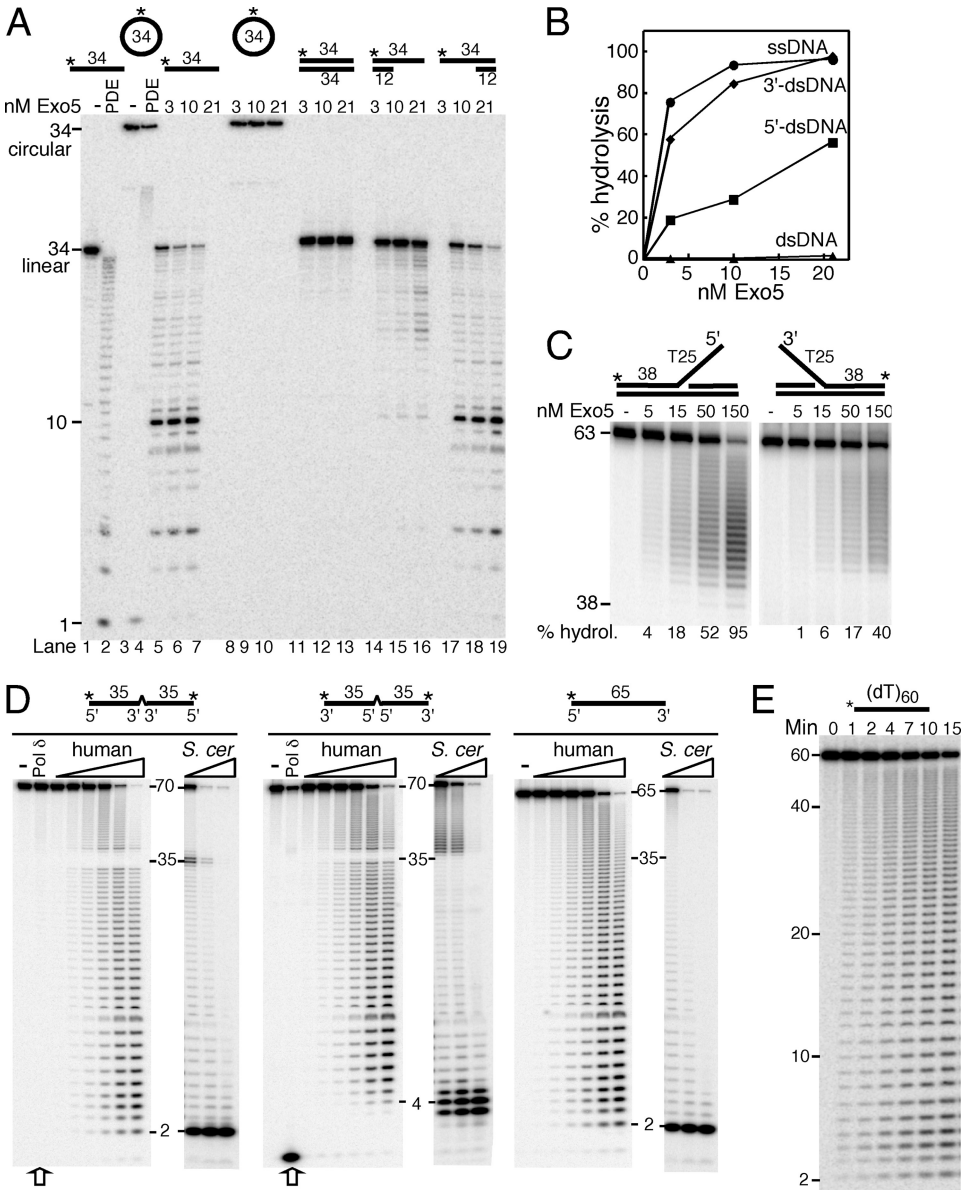

FIGURE 2. **hEXO5 is a single-stranded DNA-specific bidirectional exonuclease.** *A*, standard assays containing a 10 nM concentration of the indicated 5′-labeled DNA were incubated with 3, 10, or 21 nM hEXO5 for 8 min. *PDE*, ladder from partial digestion with snake venom phosphodiesterase, a 3′-exonuclease. *B*, quantification of activity of hEXO5 on ssDNA, dsDNA, and 5′- and 3′-dsDNA substrates from *A*. *C*, standard assays containing a 10 nM concentration of the indicated 5′- or 3′-labeled DNA substrate were incubated with 5, 15, 50, or 150 nM hEXO5 for 8 min at 30 °C. *hydrol.*, hydrolysis. *D*, standard assays containing a 10 nM concentration of 5′-labeled $(dT)_{65}$ or double 5′-ended $(dT)_{70}$, or 3′-labeled double 3′-ended $(dT)_{70}$ were incubated with 5, 15, 50, 150, or 300 nM hEXO5 for 4 min or with 0.05, 0.15, or 5 nM *S. cerevisiae* (*S. cer*) Exo5 for 30 s at 30 °C. Controls contained DNA polymerase (*Pol*) δ where indicated with an *arrow* under the gels. *E*, standard assays contained 10 nM 5′-labeled $(dT)_{60}$ and 5 nM hEXO5 for the indicated times. All samples were analyzed on 7 M urea-18% polyacrylamide gels and quantified by phosphorimaging. The *asterisks* indicate the position of the ^{32}P label.

but not the substrate with only 3′-ends (data not shown). hEXO5 degraded both polarity switch oligonucleotides, indicating that its activity is bidirectional in agreement with the studies of the flap substrates (Fig. 2*C*).

Using these diagnostic substrates, we reinvestigated the polarity preference of *S. cerevisiae* Exo5, which we previously had designated to be a 5′-exonuclease (7). Surprisingly, this enzyme also showed bidirectionality but still with a preference for 5′-ends. However, in contrast to hEXO5, which generates larger oligonucleotide products, yeast Exo5 predominantly generates dinucleotide products from the 5′-end and tri- and tetranucleotides from the 3′-end (Fig. 2*D*). We conclude that our previous inability to detect a 3′-directionality with yeast Exo5 may have been caused by the sequence context of the oligonucleotides used in that study.

Remarkably, hEXO5 releases oligonucleotides rather than mononucleotides as products of exonuclease action. The results from a single hit kinetic analysis of hEXO5 on $(dT)_{60}$ are consistent with a model in which hEXO5 loads at a DNA end and then stochastically translocates along the ssDNA prior to random cutting (Fig. 2*E*). In a single hit kinetic analysis, each DNA molecule undergoes one cleavage event upon binding by hEXO5. Under our experimental conditions, hydrolysis at early time points was <10%. Importantly, the ratio of the different length products formed between 2 and 4 min of reaction remained constant. The ratio of 2–10-nucleotide products

made after 4 min compared with 2 min of reaction time was 1.89 ± 0.2. In comparison, the ratio of 11–20-nucleotide products was 1.95 ± 0.2. Multiple cleavage events would have led to an accumulation of shorter products with increasing time. This was not observed until the 15-min time point, indicating that at the initial times single hit kinetics prevailed.

The sliding model predicts an equal probability of cutting along the length of the DNA across which sliding occurs as indeed was observed for the $(dT)_{60}$ substrate with some preference for cutting near the 5′-end, which is the preferable loading site. mEXO5 also exhibited this behavior of a sliding exonuclease (data not shown). However, *S. cerevisiae* Exo5, which functions in mitochondria, predominantly released dinucleotides as products from the 5′-end (Fig. 2*D* and Ref. 7). Therefore, the biochemistry of mammalian Exo5 is quite different from that of budding yeast Exo5.

hEXO5 Activity Is Greatly Increased by Forced Dimerization—The extremely low mammalian Exo5 catalytic activity suggests that its activity may be regulated. Interestingly, we noted that under standard assay conditions with 10 nM substrate DNA the activity of hEXO5 carrying the GST purification tag was approximately 30-fold higher than that of the protein after proteolytic removal of the GST tag (data not shown). However, the product distribution remained very similar (data not shown). We surmised that the increased activity of GST-hEXO5 was caused by the tendency of GST domains to form homodimers (10), thereby effectively dimerizing the exonuclease domain. A likely explanation for the increased activity of the dimeric enzyme would be an increased binding affinity for DNA. A full kinetic analysis of the two forms of hEXO5 showed that the native enzyme bound ssDNA over 100-fold more poorly than did GST-hEXO5 (Fig. 3*A*). At saturating ssDNA concentrations, the catalytic activities of both species differed less than 2-fold. In agreement with this conclusion, we observed no detectable binding of hEXO5 to ssDNA in an EMSA, whereas GST-hEXO5 did form a detectable complex (Fig. 3*B*). The GST domain itself showed no DNA binding (data not shown).

To determine whether the increased exonuclease activity was due to protein dimerization or a consequence of the presence of an N-terminal fusion, we reinvestigated this problem using a system of forced chemical dimerization. The N-terminal domain of the *E. coli* gyrase B subunit binds the drugs novobiocin and coumermycin with high affinity (21). Although novobiocin binds the GyrB domain in a 1:1 complex, coumermycin, which has two GyrB binding sites, forms a 1:2 complex with GyrB. We fused the GyrB domain to hEXO5 and measured its activity at 10 nM ssDNA concentrations with or without drugs (Fig. 3*C*). In the absence of antibiotic, the GyrB-hEXO5 fusion protein had very low catalytic activity similar to that of monomeric hEXO5 alone. Next, we titrated either novobiocin or coumermycin into a nuclease assay that contained a constant concentration of GyrB-hEXO5 (215 nM). The addition of increasing concentrations of novobiocin had no effect on the nuclease activity of GyrB-hEXO5. However, increasing concentrations of coumermycin led to a maximal ~10-fold increase in nuclease activity at 100 nM drug, an ~1:2 ratio of coumermycin to GyrB-hEXO5, followed by a gradual decrease in activity at higher concentrations of coumermycin (Fig. 3*C*).

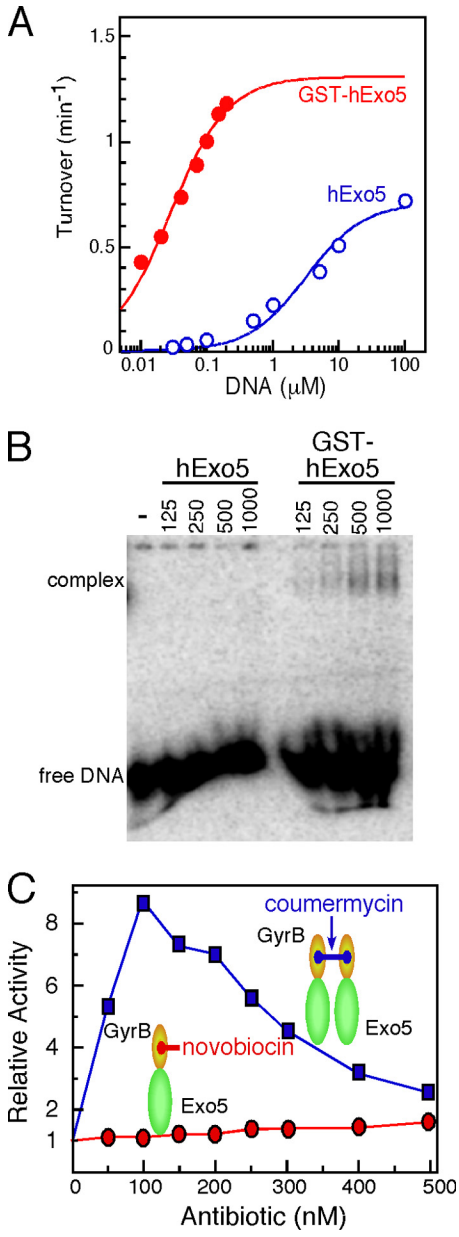

FIGURE 3. **hEXO5 possesses weak binding affinity that increases upon forced dimerization.** *A*, dependence of hEXO5 molar activity on DNA concentration. Data were fit to a Michaelis-Menten model. For GST-hEXO5, K_m = 27 ± 4 nM and V_{max} = 1.3 ± 0.05 min^{-1}; for hEXO5, K_m = 3,200 ± 800 nM and V_{max} = 0.7 ± 0.1 min^{-1}. *B*, EMSA assays as described under "Experimental Procedures" using 10 nM 5′-labeled 34-mer and the indicated concentrations of hEXO5 or GST-hEXO5 (as monomer) were incubated at 20 °C for 10 min, and samples were analyzed on a 5% non-denaturing polyacrylamide gel. Free DNA is shown. No binding was observed by GST alone (not shown). *C*, chemically enforced dimerization of hEXO5. The standard assay with 215 nM GyrB-hEXO5 was carried out with the indicated concentrations of either coumermycin or novobiocin. Novobiocin is an antibiotic that binds a single GyrB domain. Coumermycin is a dimeric antibiotic that can bind two GyrB domains as indicated.

The latter observation is consistent with a 1:2 equilibrium of coumermycin·GyrB-hEXO5 complexes that is driven to 1:1 complexes at higher coumermycin concentrations. Therefore, we conclude that high affinity DNA binding activity of hEXO5 requires that it be in the form of a dimer.

Human Replication Protein A (hRPA) Enforces a 5′-Directionality onto hEXO5—RPA is a highly conserved heterotrimeric complex that is essential for DNA replication and repair. It

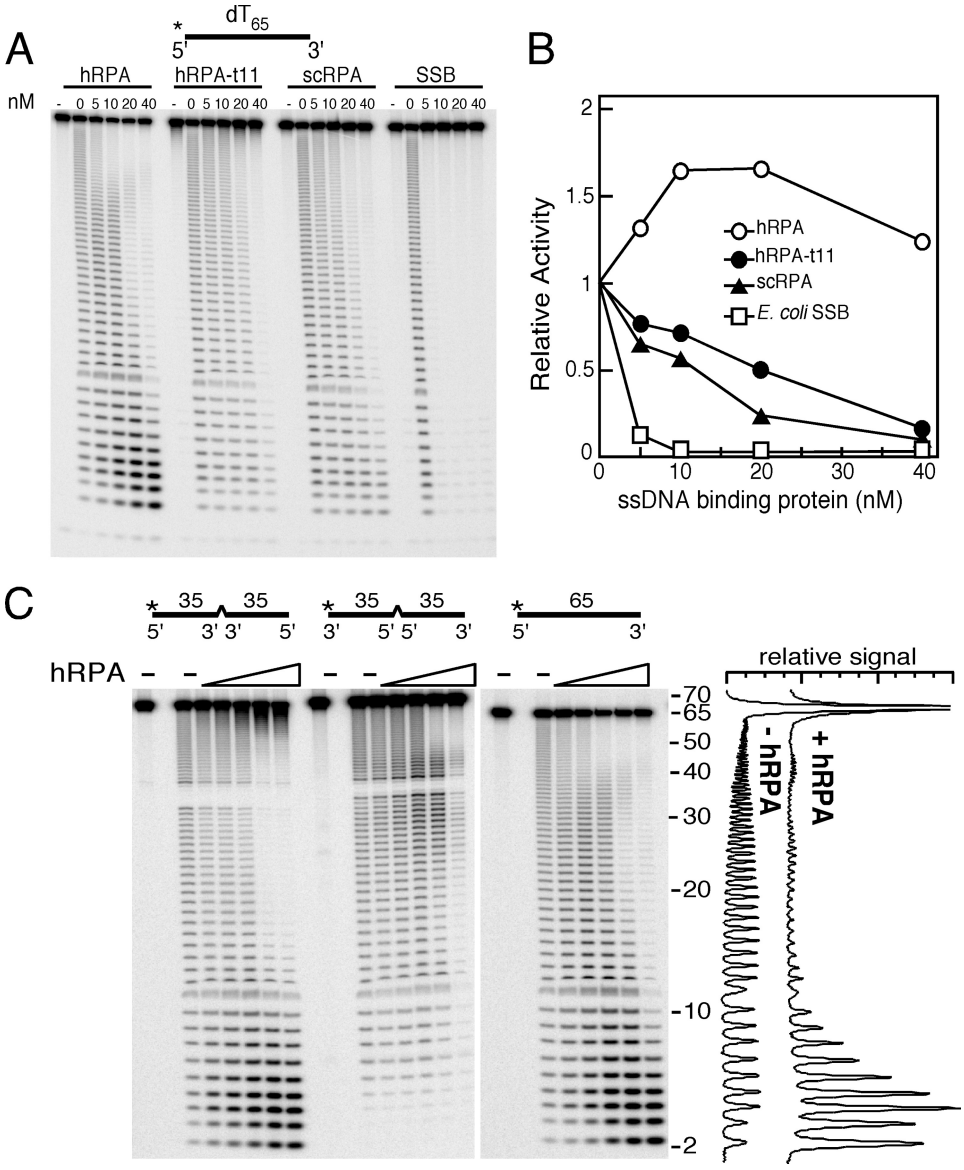

FIGURE 4. **hEXO5 is an RPA-directed 5′-exonuclease.** *A*, standard assay mixtures using 10 nM 5′-labeled $(dT)_{65}$. The concentration of the hEXO5 is 50 nM. The concentrations of WT hRPA, hRPA-t11, *S. cerevisiae* RPA (*scRPA*), and *E. coli* single-stranded DNA-binding protein (*SSB*) from *left* to *right* are 0, 5, 10, 20, and 40 nM. The reactions were carried out at 30 °C for 4 min. The results were analyzed on a 7 M urea-18% polyacrylamide gel. *B*, quantification of the gel from *A*. *C*, standard assay mixtures using 10 nM 5′-labeled $(dT)_{65}$ or $(dT)_{70}$ containing either a 3′-3′ or 5′-5′-dinucleotide linkage ssDNA substrate labeled at the 5′- or 3′-ends respectively. The concentration of the hEXO5 is 50 nM. The concentrations of human RPA from *left* to *right* are 0, 2.5, 5, 10, 20, and 40 nM. The reactions were carried out at 30 °C for 4 min. The results were analyzed on a 7 M urea-18% polyacrylamide gel. Graphs to the *right* show the distribution of hEXO5 cleavage products without hRPA or with 40 nM hRPA. The *asterisks* indicate the position of the ^{32}P label.

acts as a hub protein that recruits repair proteins to sites of DNA replication stress and DNA damage (22). To determine whether hRPA shows a functional interaction with hEXO5, we performed an activity titration experiment with increasing concentrations of either hRPA, *S. cerevisiae* RPA, or *E. coli* single-stranded DNA-binding protein on oligo$(dT)_{65}$ in the presence of a constant hEXO5 concentration. Increased coating of the ssDNA with either *S. cerevisiae* RPA or *E. coli* single-stranded DNA-binding protein progressively inhibited hEXO5 activity, whereas hRPA stimulated hEXO5 activity (Fig. 4, *A* and *B*). Therefore, hEXO5 showed notable species specificity for interaction with its cognate RPA. Remarkably, the bound RPA also curtailed the sliding ability of hEXO5. Whereas on naked $(dT)_{65}$ the probability of cutting was nearly constant over the length of the DNA, coating of the DNA with RPA shifted the cutting probability strongly toward the 5′-end (Fig. 4*C*, *right panel* and *traces*). This observation is most consistent with two simultaneous activities of hRPA. (i) It inhibits sliding of hEXO5 and stimulates cutting near the site of 5′-loading, and (ii) it inhibits 3′-loading of hEXO5.

To test this model, we used the set of oligo(dT) polarity switch oligonucleotides described in Fig. 2*D*. Coating of the 5′-double-ended substrate with hRPA enhanced activity and shifted cleavage to smaller products similarly to what was observed with the natural $(dT)_{65}$. In contrast, cutting of the 3′-double-ended substrate was strongly inhibited by hRPA (Fig. 4*C*). Thus, RPA inhibits 3′-activity of hEXO5 and thereby enforces a 5′-directionality onto the enzyme.

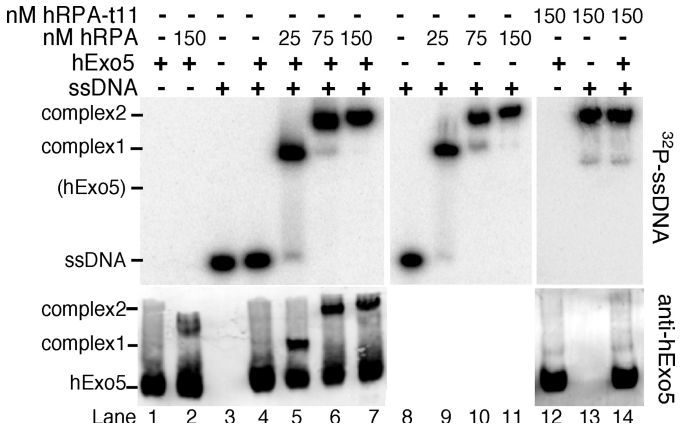

FIGURE 5. **Physical and functional interaction of hRPA with hEXO5.** EMSA assays were performed as detailed under "Experimental Procedures" using 50 nM 5′-labeled ssDNA, varying concentrations of hRPA or hRPA-t11 mutant, and 50 nM hEXO5 as indicated. The *top panel* visualizes the 5′-^{32}P-labeled oligonucleotide by phosphorimaging, and the *bottom panel* visualizes hEXO5 by a Western analysis with antibodies against hEXO5.

To further examine the specificity of the hEXO5-hRPA interaction, we took advantage of a previously characterized mutation in the N-terminal domain of the RPA70 subunit, RPA70-K45E or RPA-t11. This allele was first identified in *S. cerevisiae* as a mutant (*rfa1-t11*) that caused sensitivity to DNA damage (23), and the human mutant exhibits recombination defects (24). Mutant hRPA-t11 failed to stimulate hEXO5. In fact, it inhibited hEXO5 activity to a degree similar to that of *S. cerevisiae* RPA, suggesting that the mutation abrogated stimulatory interactions with hEXO5 (Fig. 4*A*).

We used EMSA to assess interactions among hEXO5, hRPA, and ssDNA (Fig. 5). In these studies, DNA was detected by phosphorimaging of the 5′-^{32}P label and hEXO5 by Western analysis. The $(dT)_{40}$ oligonucleotide used in this study can bind either one or two hRPAs depending on the concentration (complex 1 in *lane 9* and complex 2 in *lanes 10* and *11*). A complex between hEXO5 and hRPA was readily detectable by Western analysis (*lane 2*). Under these conditions, no complex between hEXO5 and ssDNA was detectable (*lane 4*; see also Fig. 3*B*). However, addition of increasing hRPA shifted hEXO5 into hRPA·DNA complex 1 (*lane 5*) or complex 2 (*lanes 6* and *7*). These data suggest that hEXO5 is recruited to ssDNA through binding to DNA-bound hRPA. Given the lack of stimulation of hEXO5 activity exhibited by mutant hRPA-t11 (Fig. 4*A*), we also determined interactions of the mutant protein with hEXO5. Indeed, hRPA-t11 did not form a complex with hEXO5 in the absence of DNA (compare *lanes 12* and *4*), and although hRPA-t11 alone showed robust binding to ssDNA (*lane 13*), it did not recruit hEXO5 into the RPA·ssDNA complex (compare *lanes 14* and *7*). Therefore, hRPA-t11 is defective for binding hEXO5 on or off the DNA. These data together indicate that hEXO5 physically interacts with hRPA as a mechanism to increase the affinity for ssDNA. Also, hRPA enforces 5′-directionality onto hEXO5.

hEXO5 Functions in UV Irradiation and Interstrand Cross-link Repair—Budding yeast Exo5 has a consensus mitochondrial localization signal, and the *exo5*Δ mutant shows catastrophic mitochondrial defects but no detectable nuclear defects (7). However, most other *EXO5* genes including the mammalian gene lack a mitochondrial localization signal, suggesting that their primary function may be nuclear (Fig. 1*A*). We tested the localization of a C-terminal GFP fusion to hEXO5 in transfected HEK 293 human cells. GFP fluorescence was distributed over both the cytosol and the nucleus (Fig. 6*A*). However, approximately 4 h after exposure of cells to UV irradiation, we observed distinct nuclear GFP foci, suggesting that hEXO5 is recruited to sites of DNA damage.

To determine the effect of hEXO5 on cell survival, cells with or without depletion by hEXO5-specific siRNAs were exposed to various genotoxic agents. RT-PCR was used to determine the level of hEXO5 mRNA knockdown to >80% (data not shown). Unfortunately, several independently raised antisera against purified hEXO5 failed to recognize the protein in human cell extracts. Therefore, to test the level of protein knockdown elicited by siRNAs, a FLAG-tagged hEXO5 construct containing the same RNA sequence that is targeted by the siRNAs was expressed. Extracts of hEXO5 siRNA-transfected cells were analyzed for FLAG-hEXO5 by Western analysis with anti-FLAG antibodies. From these studies, an ~80% knockdown of FLAG-tagged hEXO5 was consistently achieved (Fig. 6*B*). From these studies, we conclude that levels of native hEXO5 are similarly decreased by the siRNAs.

Treatment of hEXO5-depleted cells with DNA-damaging agents caused an increased sensitivity to various DNA-damaging agents but not to γ-irradiation as determined by clonogenic survival assays. We consider off-target effects of the siRNAs unlikely because neither siRNA1 nor siRNA2 caused an increase in sensitivity to γ-irradiation (Fig. 6*C*), but both siRNA1 and siRNA2 showed strong and similar sensitivity to treatment of cells with cisplatin (Fig. 7*A*). hEXO5 depletion in 293 cells also caused an increased sensitivity to cell killing after UV irradiation and to the alkylating agent methylmethane sulfonate (Fig. 6, *D* and *E*). An analysis of the rate of appearance and disappearance of γ-H2AX foci associated with UV damage showed a delay in their disappearance, suggesting that the rate of UV damage repair is slowed down in hEXO5-depleted cells (Fig. 6*F*).

Interestingly, hEXO5-depleted cells are very sensitive to either interstrand cross-linking agent cisplatin or MMC as determined by clonogenic survival assays (Fig. 7, *A* and *B*). Defects in ICL repair such as in Fanconi anemia patients are associated with an increase in metaphases with chromosomal aberrations. In particular, there is an increased occurrence of triradial chromosomes that is attributed to a failure in the resolution of stalled DNA replication forks (25). Indeed, we observed that chromosome abnormalities were significantly increased in hEXO5-depleted cells even in the absence of external damage-inducing agents (Fig. 7, *C*, *panel b*, *D*, and *E*). Furthermore, treatment with either interstrand cross-linking agent cisplatin (Fig. 7*D*) or mitomycin C (Fig. 7*E*) led to a large increase in the frequency of metaphases with chromosomal aberrations in hEXO5-depleted cells compared with controls. Interestingly, these included a higher frequency of triradial chromosomes (Fig. 7*C*, *panel d*). Therefore, hEXO5 depletion results in an increase in genomic instability and an increased sensitivity to various DNA-damaging agents as determined by clonogenic survival, metaphase aberrations, and appearance and disappearance of repair foci.

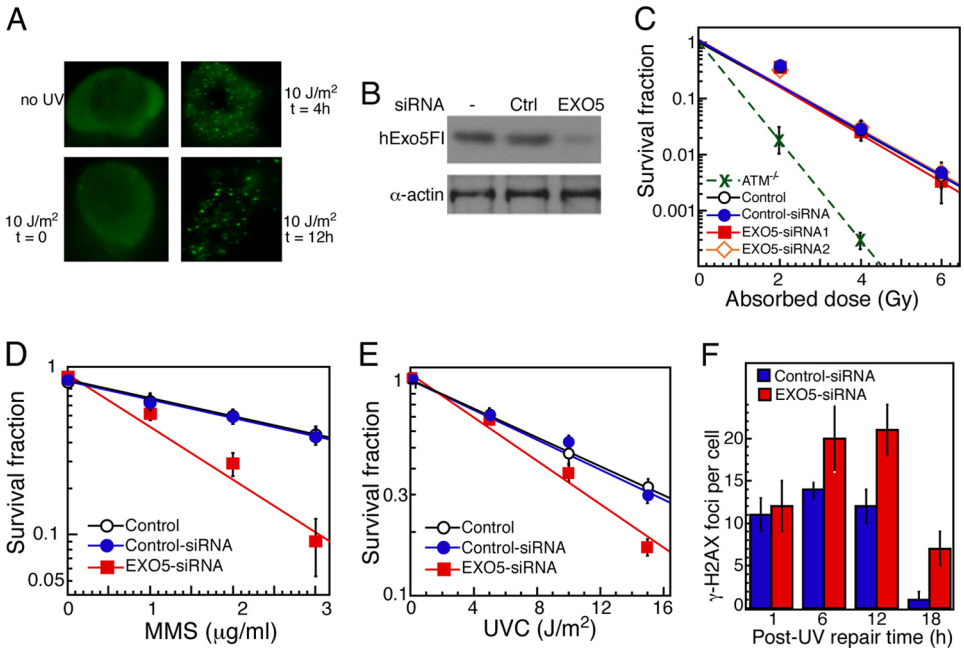

FIGURE 6. **hEXO5 is required for DNA repair.** *A*, localization. GFP-tagged hEXO5 cells were grown on coverslips, irradiated with 10 J/m^2, and examined for GFP-hEXO5 by fluorescence after the indicated times after irradiation. *B*, Western blot of FLAG-hEXO5. Human 293 cells expressing FLAG-hEXO5 were transfected with hEXO5 siRNA, and protein levels were examined 72 h after transfection. *Lane 1*, control; *lane 2*, control (*Ctrl*) siRNA; *lane 3*, hEXO5 siRNA. *C*, clonogenic survival after exposure to graded doses of ionizing radiation. *Gy*, grays. Two different siRNAs were used as indicated, and their data were virtually superimposable. An ATM$^{-/-}$ cell line was used as control. *D*, survival after exposure to methylmethane sulfonate (*MMS*). Cells were treated with methylmethane sulfonate for 4 h, washed, and incubated in fresh medium. *E*, survival after exposure to UV irradiation. *F*, frequency of γ-H2AX foci post-UV irradiation (10 J/m^2) in cells with and without depletion of hEXO5. See "Experimental Procedures" for details. *Error bars* represent S.E.

DISCUSSION

The *EXO5* gene is widely conserved in archaeal and eukaryotic organisms including mammals, fungi, plants, and protozoa; however, surprisingly, it appears to be absent from insects and worms. A phylogenetic analysis of all 95 eukaryotic complete *EXO5* genes deposited in GenBank™ shows that the proteins from organisms that fall in the Saccharomycetales order are more distantly removed from those in other orders and phyla, and they show a strong mitochondrial localization signal (Fig. 1*A*). This phylogenetic and bioinformatics analysis is supported by our experimental studies, which show severe mitochondrial but no nuclear defects for *S. cerevisiae exo5*Δ (7). In contrast, other fungi and the mammalian forms generally lack a mitochondrial localization signal, and hEXO5-depleted human cells show strong defects in nuclear genome stability.

The basic structure of Exo5 in which the N terminus is linked to its C terminus via an iron-sulfur cluster is derived from the AddB nuclease domain of the *B. subtilis* AddAB recombinase, which in turn is related to the better known *E. coli* RecBCD recombinase (8, 26). The linkage of the N terminus to the C terminus of the protein through an Fe-S cluster could provide a cavity through which the ssDNA threads. This model would explain our observation that circular ssDNA is inactive for hEXO5 (Fig. 2*A*). The Okazaki fragment-processing exonuclease Fen1 also contains a hole through which the 5′-end of the ssDNA threads, although that hole is elaborated through a flexible loop (3). Both Exo5 and Fen1 show a propensity to slide along ssDNA; however, the hydrolytic activity of Fen1 is specific for the base of a flap substrate. No such preference has been found for Exo5 (Fig. 2*C*). In fact, Exo5 is structurally related to the Dna2 nuclease-helicase, which has a similar iron-sulfur cluster arrangement (27). Another biochemical similarity between Dna2 and Exo5 is that RPA enforces a 5′–3′ directionality onto the enzyme (Fig. 4 and Ref. 28). We show here that this enforcement of directionality requires species-specific hRPA-hEXO5 interactions as neither yeast RPA nor the interaction-defective hRPA-t11 mutant fulfill this function (Figs. 4 and 5). Directionality enforcement by RPA has been demonstrated previously for enzymes and factors involved in nucleotide excision repair and in the DNA damage checkpoint, re-emphasizing the importance in carrying out these type of *in vitro* studies with the cognate form of RPA (29, 30).

What might be the biochemical role of hEXO5 during DNA repair? Given the sensitivity of hEXO5-depleted cells to UV irradiation, methylmethane sulfonate, and ICL agents, the enzyme may function in multiple pathways with partial redundancy with other nucleases. hEXO5-depleted cells are very sensitive to cisplatin and MMC, which may indicate that they have a defect in the repair of interstrand cross-links. Alternatively, because ICLs are generally detected during DNA replication (6, 31), hEXO5-depleted cells may also be defective in the processing of stalled replication forks in general. The observation that chromosome abnormalities such as triradials, which arise during S phase, are increased in hEXO5-depleted cells in the absence of damage supports this hypothesis.

Given its absolute requirement for single-stranded DNA, hEXO5 can be visualized as functioning together with a DNA helicase that generates 5′-ssDNA through unwinding or with a DNA polymerase that generates 5′-ssDNA through strand displacement synthesis. The identification of hEXO5-interacting

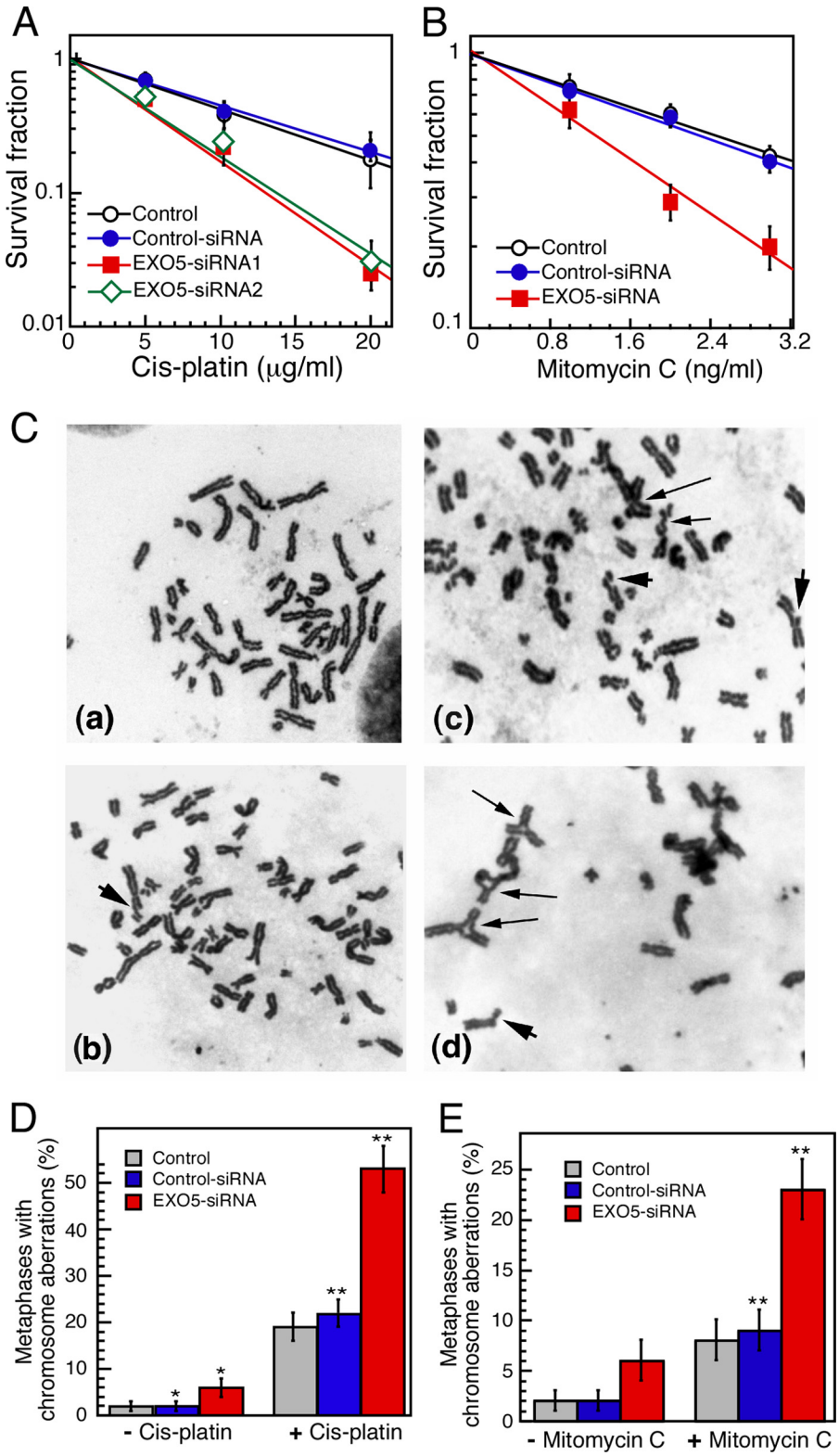

FIGURE 7. **Chromosome aberrations in hEXO5-depleted cells.** *A*, clonogenic survival of control 293 cells or those depleted for hEXO5 using either siRNA1 or siRNA2 followed by exposure to the indicated concentrations of cisplatin. *B*, survival after exposure to MMC. *C*, representative images of metaphases with chromosome aberrations. Exponentially growing cells with or without depletion of hEXO5 were treated without or with 15 μg/ml cisplatin for 1 h, cells were washed and incubated in fresh medium for 24 h, and then Colcemid was added to collect metaphases. *Thin arrows* indicate tri- or quadriradial chromosomes, and *thick arrows* indicate breaks and gaps. *Panel a*, control siRNA without cisplatin treatment; *panel b*, hEXO5 siRNA without cisplatin treatment; *panel c*, hEXO5 siRNA irradiated with 2 grays; *panel d*, hEXO5 siRNA with cisplatin treatment. *D* and *E*, histograms showing the frequency of metaphases with aberrations in control, control siRNA-, or hEXO5 siRNA-transfected cells after cisplatin (*D*) or MMC exposure (*E*) as described under "Experimental Procedures." The data presented are the mean of three experiments, and for each experiment, 100 metaphases were counted (significance according to Student's *t* test: *, $p < 0.05$; **, $p < 0.01$). *Error bars* represent S.E.

proteins beyond human RPA identified here will aid in a further understanding of the specific roles that this novel exonuclease displays during the maintenance of genome integrity. In addition, our phylogenetic analysis suggests that fission yeast Exo5 may be more closely related to the human than to the budding yeast enzyme, and in fact, a proteomics study has indicated both nuclear and mitochondrial localization for *Schizosaccharomyces pombe* Exo5 (32). We have initiated a study of Exo5 in this genetically more tractable organism.

Acknowledgments—We thank Carrie Stith for expert technical assistance in plasmid construction and protein purification, Arun Gupta for technical help, Tim Lohman for critical discussions and a gift of reverse polarity oligonucleotides, and Roberto Galletto for critical discussions and help with the analytical ultracentrifugation experiment.

REFERENCES

1. Yang, W. (2011) Nucleases: diversity of structure, function and mechanism. *Q. Rev. Biophys.* **44,** 1–93
2. Murante, R. S., Rust, L., and Bambara, R. A. (1995) Calf 5′ to 3′ exo/endonuclease must slide from a 5′ end of the substrate to perform structure-specific cleavage. *J. Biol. Chem.* **270,** 30377–30383
3. Tsutakawa, S. E., Classen, S., Chapados, B. R., Arvai, A. S., Finger, L. D., Guenther, G., Tomlinson, C. G., Thompson, P., Sarker, A. H., Shen, B., Cooper, P. K., Grasby, J. A., and Tainer, J. A. (2011) Human flap endonuclease structures, DNA double-base flipping, and a unified understanding of the FEN1 superfamily. *Cell* **145,** 198–211
4. Minko, I. G., Harbut, M. B., Kozekov, I. D., Kozekova, A., Jakobs, P. M., Olson, S. B., Moses, R. E., Harris, T. M., Rizzo, C. J., and Lloyd, R. S. (2008) Role for DNA polymerase κ in the processing of N2-N2-guanine interstrand cross-links. *J. Biol. Chem.* **283,** 17075–17082
5. Plooy, A. C., Fichtinger-Schepman, A. M., Schutte, H. H., van Dijk, M., and Lohman, P. H. (1985) The quantitative detection of various Pt-DNA-adducts in Chinese hamster ovary cells treated with cisplatin: application of immunochemical techniques. *Carcinogenesis* **6,** 561–566
6. Räschle, M., Knipscheer, P., Enoiu, M., Angelov, T., Sun, J., Griffith, J. D., Ellenberger, T. E., Schärer, O. D., and Walter, J. C. (2008) Mechanism of replication-coupled DNA interstrand crosslink repair. *Cell* **134,** 969–980
7. Burgers, P. M., Stith, C. M., Yoder, B. L., and Sparks, J. L. (2010) Yeast exonuclease 5 is essential for mitochondrial genome maintenance. *Mol. Cell. Biol.* **30,** 1457–1466
8. Yeeles, J. T., Cammack, R., and Dillingham, M. S. (2009) An iron-sulfur cluster is essential for the binding of broken DNA by AddAB-type helicase-nucleases. *J. Biol. Chem.* **284,** 7746–7755
9. Schlacher, K., Christ, N., Siaud, N., Egashira, A., Wu, H., and Jasin, M. (2011) Double-strand break repair-independent role for BRCA2 in blocking stalled replication fork degradation by MRE11. *Cell* **145,** 529–542
10. Walker, J., Crowley, P., Moreman, A. D., and Barrett, J. (1993) Biochemical properties of cloned glutathione S-transferases from *Schistosoma mansoni* and *Schistosoma japonicum*. *Mol. Biochem. Parasitol.* **61,** 255–264
11. Farrar, M. A., Alberol-Ila, J., and Perlmutter, R. M. (1996) Activation of the Raf-1 kinase cascade by coumermycin-induced dimerization. *Nature* **383,** 178–181
12. Bylund, G. O., Majka, J., and Burgers, P. M. (2006) Overproduction and purification of RFC-related clamp loaders and PCNA-related clamps from *Saccharomyces cerevisiae*. *Methods Enzymol.* **409,** 1–11
13. Pandita, R. K., Sharma, G. G., Laszlo, A., Hopkins, K. M., Davey, S., Chakhparonian, M., Gupta, A., Wellinger, R. J., Zhang, J., Powell, S. N., Roti Roti, J. L., Lieberman, H. B., and Pandita, T. K. (2006) Mammalian Rad9 plays a role in telomere stability, S- and G2-phase-specific cell survival, and homologous recombinational repair. *Mol. Cell. Biol.* **26,** 1850–1864
14. Gupta, A., Sharma, G. G., Young, C. S., Agarwal, M., Smith, E. R., Paull, T. T., Lucchesi, J. C., Khanna, K. K., Ludwig, T., and Pandita, T. K. (2005) Involvement of human MOF in ATM function. *Mol. Cell. Biol.* **25,** 5292–5305
15. Pandita, T. K., and Geard, C. R. (1996) Chromosome aberrations in human fibroblasts induced by monoenergetic neutrons. I. Relative biological effectiveness. *Radiat. Res.* **145,** 730–739
16. Pandita, T. K., Hall, E. J., Hei, T. K., Piatyszek, M. A., Wright, W. E., Piao, C. Q., Pandita, R. K., Willey, J. C., Geard, C. R., Kastan, M. B., and Shay, J. W. (1996) Chromosome end-to-end associations and telomerase activity during cancer progression in human cells after treatment with α-particles simulating radon progeny. *Oncogene* **13,** 1423–1430
17. Gupta, A., Yang, Q., Pandita, R. K., Hunt, C. R., Xiang, T., Misri, S., Zeng, S., Pagan, J., Jeffery, J., Puc, J., Kumar, R., Feng, Z., Powell, S. N., Bhat, A., Yaguchi, T., Wadhwa, R., Kaul, S. C., Parsons, R., Khanna, K. K., and Pandita, T. K. (2009) Cell cycle checkpoint defects contribute to genomic instability in PTEN deficient cells independent of DNA DSB repair. *Cell Cycle* **8,** 2198–2210
18. Hunt, C. R., Pandita, R. K., Laszlo, A., Higashikubo, R., Agarwal, M., Kitamura, T., Gupta, A., Rief, N., Horikoshi, N., Baskaran, R., Lee, J. H., Löbrich, M., Paull, T. T., Roti Roti, J. L., and Pandita, T. K. (2007) Hyperthermia activates a subset of ataxia-telangiectasia mutated effectors independent of DNA strand breaks and heat shock protein 70 status. *Cancer Res.* **67,** 3010–3017
19. Pandita, T. K., Westphal, C. H., Anger, M., Sawant, S. G., Geard, C. R., Pandita, R. K., and Scherthan, H. (1999) Atm inactivation results in aberrant telomere clustering during meiotic prophase. *Mol. Cell. Biol.* **19,** 5096–5105
20. Singleton, M. R., Dillingham, M. S., Gaudier, M., Kowalczykowski, S. C., and Wigley, D. B. (2004) Crystal structure of RecBCD enzyme reveals a machine for processing DNA breaks. *Nature* **432,** 187–193
21. Farrar, M. A., Olson, S. H., and Perlmutter, R. M. (2000) Coumermycin-induced dimerization of GyrB-containing fusion proteins. *Methods Enzymol.* **327,** 421–429
22. Binz, S. K., Sheehan, A. M., and Wold, M. S. (2004) Replication protein A phosphorylation and the cellular response to DNA damage. *DNA Repair* **3,** 1015–1024
23. Umezu, K., Sugawara, N., Chen, C., Haber, J. E., and Kolodner, R. D. (1998) Genetic analysis of yeast RPA1 reveals its multiple functions in DNA metabolism. *Genetics* **148,** 989–1005
24. Kantake, N., Sugiyama, T., Kolodner, R. D., and Kowalczykowski, S. C. (2003) The recombination-deficient mutant RPA (rfa1-t11) is displaced slowly from single-stranded DNA by Rad51 protein. *J. Biol. Chem.* **278,** 23410–23417
25. D'Andrea, A. D. (2010) Susceptibility pathways in Fanconi's anemia and breast cancer. *N. Engl. J. Med.* **362,** 1909–1919
26. Saikrishnan, K., Yeeles, J. T., Gilhooly, N. S., Krajewski, W. W., Dillingham, M. S., and Wigley, D. B. (2012) Insights into Chi recognition from the structure of an AddAB-type helicase-nuclease complex. *EMBO J.* **31,** 1568–1578
27. Pokharel, S., and Campbell, J. L. (2012) Cross talk between the nuclease and helicase activities of Dna2: role of an essential iron-sulfur cluster domain. *Nucleic Acids Res.* **40,** 7821–7830
28. Nimonkar, A. V., Genschel, J., Kinoshita, E., Polaczek, P., Campbell, J. L., Wyman, C., Modrich, P., and Kowalczykowski, S. C. (2011) BLM-DNA2-RPA-MRN and EXO1-BLM-RPA-MRN constitute two DNA end resection machineries for human DNA break repair. *Genes Dev.* **25,** 350–362
29. de Laat, W. L., Appeldoorn, E., Sugasawa, K., Weterings, E., Jaspers, N. G., and Hoeijmakers, J. H. (1998) DNA-binding polarity of human replication protein A positions nucleases in nucleotide excision repair. *Genes Dev.* **12,** 2598–2609
30. Majka, J., Binz, S. K., Wold, M. S., and Burgers, P. M. (2006) Replication protein A directs loading of the DNA damage checkpoint clamp to 5′-DNA junctions. *J. Biol. Chem.* **281,** 27855–27861
31. Knipscheer, P., Räschle, M., Smogorzewska, A., Enoiu, M., Ho, T. V., Schärer, O. D., Elledge, S. J., and Walter, J. C. (2009) The Fanconi anemia pathway promotes replication-dependent DNA interstrand cross-link repair. *Science* **326,** 1698–1701
32. Matsuyama, A., Arai, R., Yashiroda, Y., Shirai, A., Kamata, A., Sekido, S., Kobayashi, Y., Hashimoto, A., Hamamoto, M., Hiraoka, Y., Horinouchi, S., and Yoshida, M. (2006) ORFeome cloning and global analysis of protein localization in the fission yeast *Schizosaccharomyces pombe*. *Nat. Biotechnol.* **24,** 841–847